Short communication

Effect of Ti addition to Pt/C catalyst on methanol electro-oxidation and oxygen electro-reduction reactions

Min Ku Jeon, Paul J. McGinn*

Department of Chemical and Biomolecular Eng., University of Notre Dame, 178 Fitzpatrick, Notre Dame, IN 46556, USA

ARTICLE INFO

ABSTRACT

Carbon supported binary Pt–Ti alloys were investigated for application in methanol electro-oxidation (MOR) and oxygen electro-reduction reactions (ORR). Various compositions of $Pt_{100-x}Ti_x$/C ($x = 0$, 25, 50, and 75) catalysts were synthesized by sequential impregnation of Pt and Ti followed by annealing at 900 °C for 30 min under H_2/Ar flow. X-ray diffraction results showed formation of the Pt_3Ti intermetallic phase in $Pt_{50}Ti_{50}$ and $Pt_{25}Ti_{75}$ catalysts after annealing at 900 °C. The $Pt_{50}Ti_{50}$/C-900 and $Pt_{25}Ti_{75}$/C-900 catalysts (the '-900' designation indicates the catalyst was annealed at 900 °C) exhibited 103% ($87.4\,mA\,mg_{Pt}^{-1}$) and 198% ($128\,mA\,mg_{Pt}^{-1}$) higher MOR activity, respectively, than in the Pt/C-900 catalyst ($43.0\,mA\,mg_{Pt}^{-1}$) at 0.7 V (vs. reversible hydrogen electrode (RHE)). These two catalysts also showed high ORR activity. From a specific activity basis, the $Pt_{50}Ti_{50}$/C-900 and $Pt_{25}Ti_{75}$/C-900 catalysts exhibited 32.3 and $30.2\,\mu A\,cm_{Pt}^{-2}$, respectively, which were 171 and 154% higher than the $11.9\,\mu A\,cm_{Pt}^{-2}$ value of the Pt/C catalyst at 0.8 V (vs. RHE). Methanol-tolerant ORR activity was also investigated, but in the presence of methanol, the $Pt_{50}Ti_{50}$/C-900 and $Pt_{25}Ti_{75}$/C-900 catalysts both exhibited poor ORR activity.

© 2009 Elsevier B.V. All rights reserved.

1. Introduction

The methanol electro-oxidation reaction (MOR) is under intensive research due to its application in direct methanol fuel cells (DMFCs) [1]. Pt was first introduced as the MOR catalyst in DMFCs, but poor CO tolerance prohibited its commercial application. Currently the state-of-the-art catalyst is a binary PtRu alloy which can oxidize CO at relatively lower potential than pure Pt, but the PtRu catalyst still suffers from high cost and low catalytic activity [2–5]. There have been various efforts aimed at solving these problems. Most of the reported research has been focused on transition metal doped PtRu catalysts [6–8], including ternary PtRuFe [9,10], PtRuCo [11–13], PtRuNi [14,15], and PtRuCu [16] catalysts. Although these PtRu-based ternary catalysts have achieved cost reduction and activity improvement, dissolution of Ru still remains as an obstacle [17–20]. As an alternative, Pt-based binary alloys have also been investigated, and promising results have been reported in PtBi [21], PtPb [21,22], and PtTi [23] catalysts.

The oxygen electro-reduction reaction (ORR) is also of great interest because of its application in both DMFC and polymer electrolyte membrane fuel cells [24]. For the ORR, pure Pt is widely used, but due to the same reasons as for the PtRu catalyst (high cost and low activity), improvement of the pure Pt catalyst is desirable.

Alloying Pt with transition metals such as Fe [25,26], Ni [27–29], Co [28,29], and Ti [30] has been shown to achieve both goals of cost reduction and activity improvement. The positive effect of alloying Pt with transition metals is generally explained by two effects: (1) an electronic effect (Pt d-band vacancy modification) [27,31–34] and (2) a geometric effect (contraction of Pt–Pt bonding distance leading to a favorable condition for the ORR) [34,35].

In the present study, we examine Ti as a promoter of Pt catalyst activity because it was identified as a promising candidate for improving both the MOR [23,36,37] and ORR activity [30,38]. As early as 1976, Janssen and Moolhuysen [36] reported a Pt–Ti alloy as a promising catalyst for the MOR. Hamnett et al. [37] reported that TiO_2 acts as a promoter for the MOR at low current densities while it acts as an inhibitor at high current densities. A Pt_3Ti catalyst investigated by Abe et al. [23] exhibited higher MOR activity than PtRu and Pt catalysts. In addition, they claimed that ordered Pt_3Ti phase exhibited higher MOR activity than disordered Pt_3Ti. For the ORR, Ding et al. [30] reported that they could achieve a twofold improvement over the ORR activity of pure Pt with a $Pt_{75}Ti_{25}$ catalyst. They observed the Pt_3Ti phase in their $Pt_{75}Ti_{25}$ catalyst, but the role of the Pt_3Ti phase was not clear as they could not obtain 100% ordered Pt_3Ti phase even after 950 °C annealing. A $Pt–TiO_2$/C catalyst was also reported to exhibit higher ORR activity than pure Pt/C catalyst [38]. Xiong and Manthiram [39] reported that a Pt/TiO_x/C catalyst showed higher ORR activity than Pt in the presence of methanol. These reports suggest that Pt–Ti alloys merit further investigation for application as MOR and ORR catalysts.

The most popular method to synthesize nanometer sized electrocatalysts is through chemical reduction methods (such as impregnation method, colloidal method, micro-emulsion method, and polyol method) because they do not require high temperature annealing which causes particle size increase [5,40]. Unfortunately Ti-containing electrocatalysts cannot be synthesized via normal chemical reduction routes due to the high oxyphilic characteristic of Ti [41]. Successful synthesis of Pt–Ti binary alloys was achieved by synthesizing the catalysts under oxygen-free conditions [23,30]. In the present study, we deposited Pt and Ti sequentially and then heat treated at 900 °C to form Pt–Ti binary alloys. The prepared catalysts were characterized for their structural and electrochemical properties including MOR and ORR activities. For the ORR activity, the effect of methanol tolerance was also investigated to verify the feasibility of the Pt–Ti catalysts for application in a DMFC cathode, which requires methanol tolerance in addition to high ORR activity because of methanol cross-over [1].

2. Experimental

2.1. Synthesis of catalysts

First, Pt was deposited on a carbon support (Vulcan XC-72R) by the impregnation method using $NaBH_4$ as a reduction agent. Briefly, H_2PtCl_6 was dissolved in a mixture of de-ionized (DI) water and methanol. The carbon support was added to the solution and then put through sonication for dispersion. The mixture was further stirred for 30 min and then Pt was reduced by adding 0.2 M $NaBH_4$ solution to the mixture. The resulting mixture was further stirred for 1 h to confirm termination of reduction. The Pt/C catalyst was obtained by filtering and washing the resulting powder with DI water. The Pt/C catalyst was dried at 100 °C in an oven overnight. The amount of Pt was adjusted to 20 wt.% (carbon support + Pt). Incorporation of Ti was performed by using the Pt/C catalyst as a starting material. An appropriate amount of Ti acetylacetonate (Ti(acac), 75% Ti chelate in isopropyl alcohol) solution was added to the Pt/C catalyst. The mixture was dried at 100 °C for 2 h to remove the solvent of the Ti(acac) solution. The dried powder was annealed at 900 °C for 30 min in flowing H_2/Ar (5.2 mol.% H_2). By adjusting the amount of Ti(acac) solution added to the Pt/C catalyst, various compositions were prepared (Pt/C-900, $Pt_{75}Ti_{25}$/C-900, $Pt_{50}Ti_{50}$/C-900, $Pt_{25}Ti_{75}$/C-900, and Ti/C-900 corresponding to the Pt:Ti molar ratio). The designation '-900' at the end of the catalyst names indicates that the catalysts were annealed at 900 °C for 30 min as noted above.

2.2. Structural and electrochemical characterization of the catalysts

Structural properties of the catalysts were characterized by collecting X-ray diffraction (XRD) data over a 2θ range between 20° and 80° in a step scan mode. A 0.02° step was employed with 0.5 s counting time for each step.

A rotating disk electrode (RDE) technique was employed for electrochemical analysis of the catalysts. To make a thin film of the catalysts on a glassy carbon electrode (dia.: 0.45 cm), catalyst dispersions were prepared by adding DI water and 5 wt.% Nafion ionomer solution (2:10 volume ratio) to a certain amount of catalyst powder. The dispersion was sonicated to get homogeneous mixing, and then 10 μL of the dispersion was dripped on the glassy carbon electrode. Catalyst loading on the RDE electrode was $0.524\,mg_{catal.}\,cm^{-2}$. The thin film electrode was dried in air before being tested. Cyclic voltammetry (CV) was performed by potential cycling between 0 and 1.2 V (vs. reversible hydrogen electrode (RHE)) for 50 cycles at a scan rate of $50\,mV\,s^{-1}$. Nitrogen purged 0.5 M H_2SO_4 solution was used as the electrolyte. MOR activity

was measured by potential cycling between 0 and 0.8 V (vs. RHE) at a scan rate of $50\,mV\,s^{-1}$ in 1 M H_2SO_4 + 1 M methanol solution. ORR activity was measured by a cathodic potential sweep from 1.0 to 0.2 V (vs. RHE) at a scan rate of $5\,mV\,s^{-1}$. Methanol tolerance was evaluated by employing both (0.5 M H_2SO_4) and (0.5 M H_2SO_4 + 0.1 M methanol) solutions as the electrolyte for the ORR activity testing. Rotation speed of the RDE during the ORR activity measurement was 2000 rpm. All potentials in this paper were converted into RHE scale.

3. Results and discussion

Fig. 1(a) shows the XRD patterns of the synthesized catalysts. In the $Pt_{75}Ti_{25}$/C-900 catalyst, we could not observe any new peaks except for the fcc Pt peaks. However, the 2θ position of the (1 1 1) peak slightly moved from 39.70° in the Pt/C-900 catalyst to 39.74° in the $Pt_{75}Ti_{25}$/C-900 catalyst. This result indicates that little if any alloying was achieved in the $Pt_{75}Ti_{25}$/C-900 catalyst, because the shift (0.04°) is not much different from the experimental resolution of the XRD data (0.02° step). In the $Pt_{50}Ti_{50}$/C-900 catalyst, new peaks were observed at 22.8° and 32.5°, which match with the (1 0 0) and (1 1 0) peaks of the cubic Pt_3Ti phase (ICDD 62-3259) as shown in Fig. 1(b). These peaks were also observed in the $Pt_{27}Ti_{75}$/C-900 catalyst, as shown in inset of Fig. 1(a), which was acquired with a longer counting time for each step to obtain improved data. The broad peak near 25° came from the carbon support, which overlaps with the Pt_3Ti (1 0 0) peak. Although the peaks are not intense, the XRD results show the existence of the ordered Pt_3Ti phase in both the $Pt_{50}Ti_{50}$/C-900 and $Pt_{25}Ti_{75}$/C-900 catalysts. This result is in accordance with a previous report [42]. Beard and Ross Jr. [42] claimed that a Pt–TiO_2 mixture could be transformed
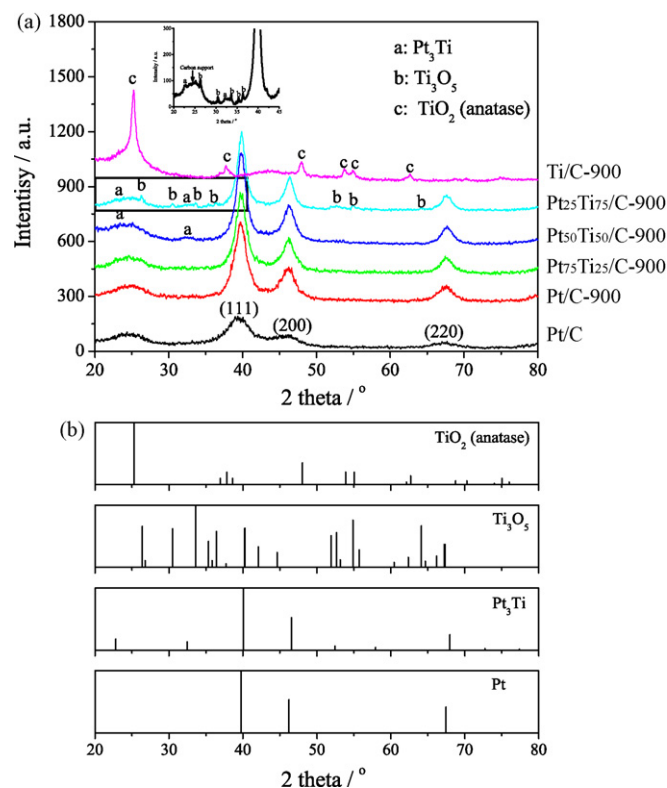

Fig. 1. (a) The XRD patterns of Pt/C, Pt/C-900, $Pt_{75}Ti_{25}$/C-900, $Pt_{50}Ti_{50}$/C-900, $Pt_{25}Ti_{75}$/C-900, and Ti/C-900 catalysts. Inset shows a portion of the $Pt_{25}Ti_{75}$/C-900 XRD pattern (in the outlined box) measured with a longer counting time (3 s step^{-1}). (b) Peak positions and intensities of Pt (ICDD 65-2868), Pt_3Ti (ICDD 65-3259), Ti_3O_5 (ICDD 40-0806), and TiO_2 (anatase, ICDD 21-1272).

Table 1
A summary of structural properties of the Pt–Ti binary catalysts.

	(1 1 1) peak position (°)	d (nm)	Lattice parameter (nm)	Crystallite size (nm)
Pt/C	39.41	0.2285	0.3958	2.4
Pt/C-900	39.70	0.2269	0.3930	4.2
$Pt_{75}Ti_{25}$/C-900	39.74	0.2266	0.3925	5.1
$Pt_{50}Ti_{50}$/C-900	39.77	0.2265	0.3923	5.7
$Pt_{25}Ti_{75}$/C-900	39.81	0.2262	0.3918	6.7

Table 2
A summary of electrochemical testing results of the Pt–Ti binary catalysts.

	MOR activity at 0.7 V (vs. RHE)		ORR activity at 0.8 V (vs. RHE)			
	Mass activity ($mA\ mg_{Pt}^{-1}$)	Specific activity ($\mu A\ cm_{Pt}^{-2}$)	RDE current density ($mA\ cm^{-2}$)	Mass activity ($mA\ mg_{Pt}^{-1}$)	Specific activity ($\mu A\ cm_{Pt}^{-2}$)	Current density decrease by the presence of methanol ($mA\ cm^{-2}$)
Pt/C	127	197	0.807	7.71	11.9	1.01
Pt/C-900	41.8	88.7	0.681	6.50	13.8	0.642
$Pt_{75}Ti_{25}$/C-900	42.2	99.1	0.660	6.40	15.0	0.821
$Pt_{50}Ti_{50}$/C-900	69.4	211	1.00	10.6	32.3	1.63
$Pt_{25}Ti_{75}$/C-900	104.2	262	1.10	12.0	30.2	1.47

into the Pt_3Ti phase by annealing at 900–1200 °C under He flow. It also should be noted that Pt_3Ti peaks were not observed in the $Pt_{75}Ti_{25}$/C-900 catalyst although it is an identical composition with the Pt_3Ti phase. It can be the results of two causes: (1) the synthesis method employed in the present study cannot guarantee good mixing of Pt and Ti, as Ti could have been deposited separate from the Pt particles so that they cannot form alloys and (2) literature suggests this phase does not readily form. Only a small amount of ordered Pt_3Ti phase was formed as reported by Abe et al. [23] and Ding et al. [30]. Abe et al. [23] could obtain fully ordered Pt_3Ti phase in $Pt_{50}Ti_{50}$ composition. Ding et al. [30] could observe XRD peaks of ordered Pt_3Ti phase in their $Pt_{75}Ti_{25}$/C catalyst after annealing at 850 and 950 °C, but even after 950 °C annealing, the concentration of Pt_3Ti intermetallic phase was only 76% of the total metal content. In the $Pt_{25}Ti_{75}$/C-900 catalyst, additional peaks were observed, which were assigned as a Ti_3O_5 phase. This is an interesting result as only anatase TiO_2 peaks could be observed in the Ti/C-900 catalysts. The presence of Ti_3O_5 suggests that the excess TiO_2 was partially reduced in the presence of Pt as it was not observed in the Ti/C-900 catalyst. In addition, the absence of anatase TiO_2 peaks in the Pt–Ti binary catalysts indicates that the amount of isolated Ti oxides from Pt caused by two step synthesis is relatively small [38]. Therefore, the XRD results show that the Pt–Ti catalysts are mixtures of Pt, Pt_3Ti, Ti_3O_5, and small amount of TiO_2. It should be noted that structural changes were observed in the Pt/C catalyst after 900 °C annealing. As shown in Table 1, the (1 1 1) peak position

of the Pt/C catalyst moved from 39.41° to 39.70° after annealing, which indicates contraction of Pt–Pt distance was caused during the annealing. When we consider that the reference standard peak position is 39.75° (ICDD 65-2868), this result suggests that the $NaBH_4$ reduced Pt catalyst (Pt/C) was not fully ordered and contains some amorphous Pt. The size of the platinum crystallites of the catalysts was determined by employing the Scherrer equation [43] on the (1 1 1) peak, giving results of 2.4, 4.2, 5.1, 5.7, and 6.7 nm for the Pt/C, Pt/C-900, $Pt_{75}Ti_{25}$/C, $Pt_{50}Ti_{50}$/C, and $Pt_{25}Ti_{75}$/C catalysts, respectively. The XRD results are summarized in Table 1.

The CV results are shown in Fig. 2. With increasing Ti content, a decrease of current densities for hydrogen adsorption/desorption (0–0.3 V) and Pt oxidation (0.8–1.2 V)/reduction (ca. 0.7 V) was observed. Significant changes were not observed in the CV results, indicating that structural changes observed in the XRD results did not affect the CV performance significantly. Electrochemically active surface area (EAS) was calculated from the hydrogen desorption peak area (0–0.3 V along the positive scan) to compare intrinsic activity of the catalysts. For the calculation of EAS, $210\ \mu C\ cm^{-2}$ was assumed as the monolayer charge [44]. It should be noted that the EAS calculation based on the hydrogen desorption area is not a precise method in alloy catalysts, but it is still useful in comparing relative activities. The calculated EAS values were 64.5, 47.1, 42.6, 32.9, and $39.8\ m^2\ g_{Pt}^{-1}$ for the Pt/C, Pt/C-900, $Pt_{75}Ti_{25}$/C-900, $Pt_{50}Ti_{50}$/C-900, and $Pt_{25}Ti_{75}$/C-900 catalysts, respectively. The relative decrease in EAS values was not as much as the decrease in the Pt content, which suggests that some of Ti oxides are not in contact with Pt as discussed above.

Fig. 3(a) shows the MOR activity (current density) on the basis of Pt mass ($mA\ mg_{Pt}^{-1}$). In the forward scan direction, the Pt/C catalyst showed the highest MOR activity of $127\ mA\ mg_{Pt}^{-1}$ at 0.7 V. In the Pt/C-900 catalyst, the mass activity significantly decreased to $41.8\ mA\ mg_{Pt}^{-1}$ due to a particle size increase and the formation of the ordered phase. The MOR activity of the $Pt_{75}Ti_{25}$/C-900 catalyst ($42.2\ mA\ mg_{Pt}^{-1}$) was very close to that of the Pt/C-900 catalyst. The $Pt_{50}Ti_{50}$/C-900 catalyst showed significantly increased MOR activity ($69.4\ mA\ mg_{Pt}^{-1}$) that was 66% higher than that of the Pt/C-900 catalyst. The MOR activity further increased in the $Pt_{25}Ti_{75}$/C catalyst to $104\ mA\ mg_{Pt}^{-1}$, which is 149% higher than $41.8\ mA\ mg_{Pt}^{-1}$ of the Pt/C-900 catalyst. The improvement of the MOR activity with Ti additions is more clearly illustrated on a specific activity scale ($\mu A\ cm_{Pt}^{-2}$), as shown in Fig. 3(b). This figure was obtained by normalizing Fig. 3(a) with the EAS values. The specific activities at 0.7 V were 197, 88.7, 99.1, 211, and $262\ \mu A\ cm_{Pt}^{-2}$ for the Pt/C, Pt/C-900, $Pt_{75}Ti_{25}$/C-900, $Pt_{50}Ti_{50}$/C-900, and $Pt_{25}Ti_{75}$/C-900
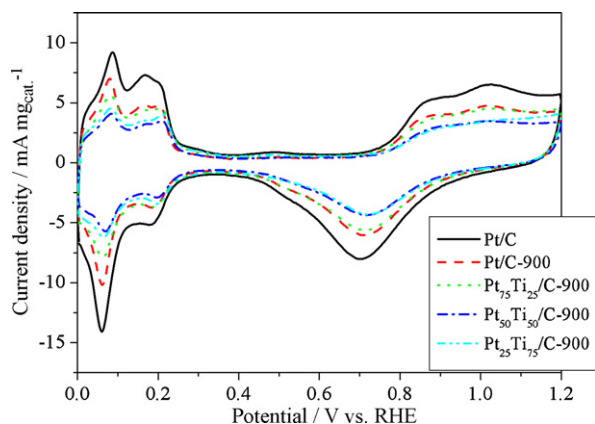

Fig. 2. The CV results of Pt/C, Pt/C-900, and Pt–Ti binary catalysts. Testing was performed in nitrogen purged 0.5 M H_2SO_4 solution by potential cycling between 0 and 1.2 V at a scan rate of $50\ mV\ s^{-1}$.
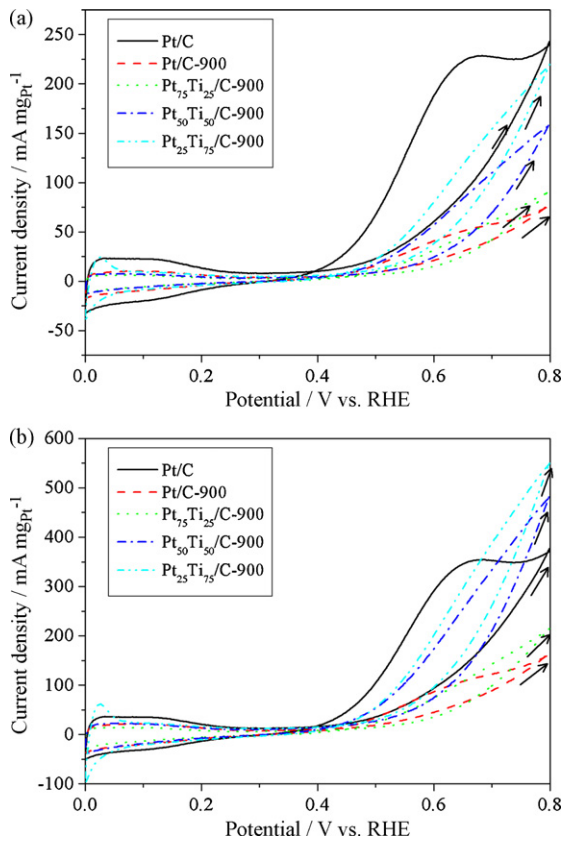
Fig. 3. The MOR activity measurement results shown in (a) mass activity (mA mg_{Pt}^{-1}) and (b) specific activity ($\mu A\ cm_{Pt}^{-2}$) scale. The experiment was performed by potential cycling between 0 and 0.8 V at a scan rate of 50 mV s^{-1} in nitrogen purged 1 M H$_2$SO$_4$ + 1 M methanol solution.

catalysts, respectively. The specific activities of the Pt$_{50}$Ti$_{50}$/C-900 and Pt$_{25}$Ti$_{75}$/C-900 catalysts were 138 and 195% higher than that of the Pt/C-900 catalyst, respectively, while that of the Pt$_{75}$Ti$_{25}$/C catalyst was only 12% better. The MOR activity testing results are summarized in Table 2. As previous reports have suggested that both TiO$_2$ [38] and formation of the Pt$_3$Ti phase [23] can improve the MOR activity, it is not clear whether either or both of them caused the significant increase of the MOR activity in the Pt$_{50}$Ti$_{50}$/C-900 and Pt$_{25}$Ti$_{75}$/C-900 catalysts. But these results clearly show positive effect of Ti additions to Pt catalyst for the MOR. Here, it would be helpful to compare these results with a previous report [23]. Abe et al. [23] reported that they could achieve about 23 times higher MOR activity in their ordered Pt$_3$Ti catalyst at 0.82 V than that of pure Pt. Their improvement is much larger than we observed in this paper, which might have resulted from the different synthesis method, the degree of alloying, and the structure of the catalysts, including existence of TiO$_2$ and the nature of the carbon support.

Fig. 4(a) shows the RDE test results for ORR activity measurements. Current densities at 0.8 V are shown in Fig. 4(b) and Table 2 for convenient comparison. At 0.8 V, the current densities of the Pt/C-900 and Pt$_{75}$Ti$_{25}$/C-900 catalysts were 0.681 and 0.660 mA cm^{-2}, respectively, which were lower than 0.807 mA cm^{-2} of the Pt/C catalyst. But the Pt$_{50}$Ti$_{50}$/C-900 and Pt$_{25}$Ti$_{75}$/C-900 catalysts exhibited improved ORR activity of 1.06 and 1.1 mA cm^{-2}, respectively. Further comparison was made in terms of mass activity (mA mg$_{Pt}^{-1}$) and specific activity ($\mu A\ cm_{Pt}^{-2}$) of the catalysts as shown in Fig. 4(c) and Table 2. In terms of specific activity, the change of the ORR activity was significant. The specific activity of the Pt$_{75}$Ti$_{25}$/C catalyst only slightly increased to 15.0 $\mu A\ cm_{Pt}^{-2}$ compared with 11.9 and 13.8 $\mu A\ cm_{Pt}^{-2}$ values of
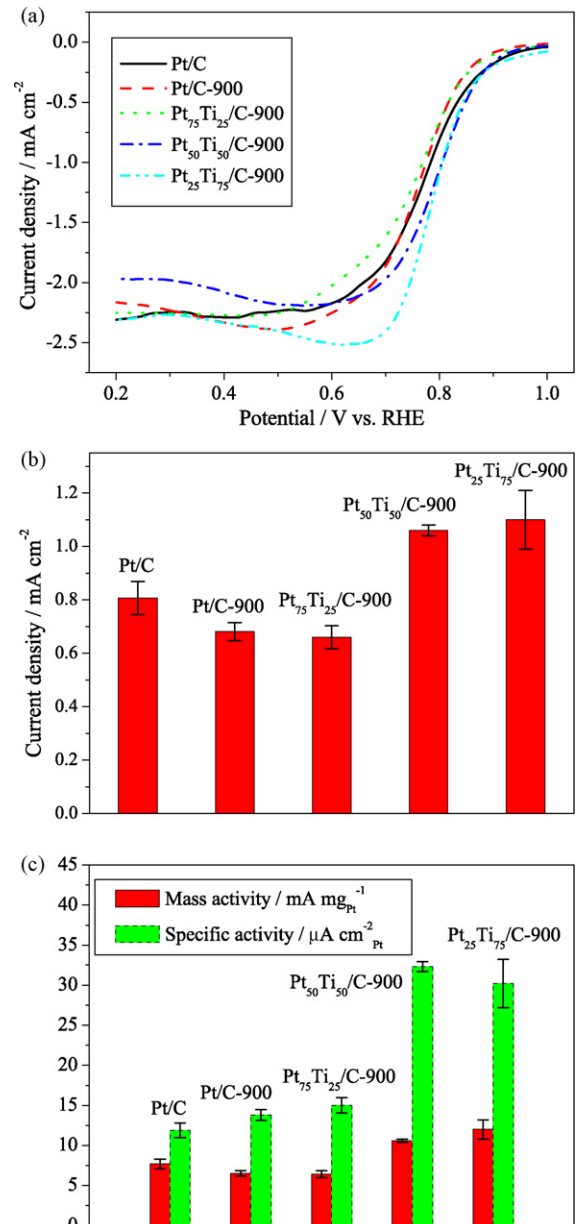

Fig. 4. (a) The RDE test results performed by cathodic potential sweep from 1.0 to 0.2 V at a scan rate of 5 mV s^{-1}. Oxygen purged 0.5 M H$_2$SO$_4$ solution was used as the electrolyte. Rotating speed of the RDE was 2000 rpm. (b) Current densities of the catalysts at 0.8 V. (c) The ORR activity of the catalyst at 0.8 V shown in mass (mA mg$_{Pt}^{-2}$) and specific ($\mu A\ cm_{Pt}^{-2}$) scale.

the Pt/C and Pt/C-900 catalysts, respectively. However, the ORR specific activity significantly increased (more than twice the Pt/C and Pt/C-900 catalysts values) to 32.3 and 30.2 $\mu A\ cm_{Pt}^{-2}$ in the Pt$_{50}$Ti$_{50}$/C-900 and Pt$_{25}$Ti$_{75}$/C-900 catalysts, respectively. Like the MOR activity results, one cannot unambiguously conclude whether the high ORR activities came from TiO$_2$ or Pt$_3$Ti formation. Based on the previous reports [23,30,36–38], either the Pt$_3$Ti phase or Ti oxides might have contributed to improvement of the MOR and ORR activities. In the present study, improvement in the ORR mass activity in the Pt$_{25}$Ti$_{75}$/C-900 catalyst was 62 and 36% higher than those of Pt/C-900 and Pt/C catalysts, respectively. This improvement is not as high as the 100% improvement reported by Ding et al. [30], which might have been caused by the different synthesis method used and the resulting structure of the catalysts including the degree of alloying and existence of TiO$_2$.
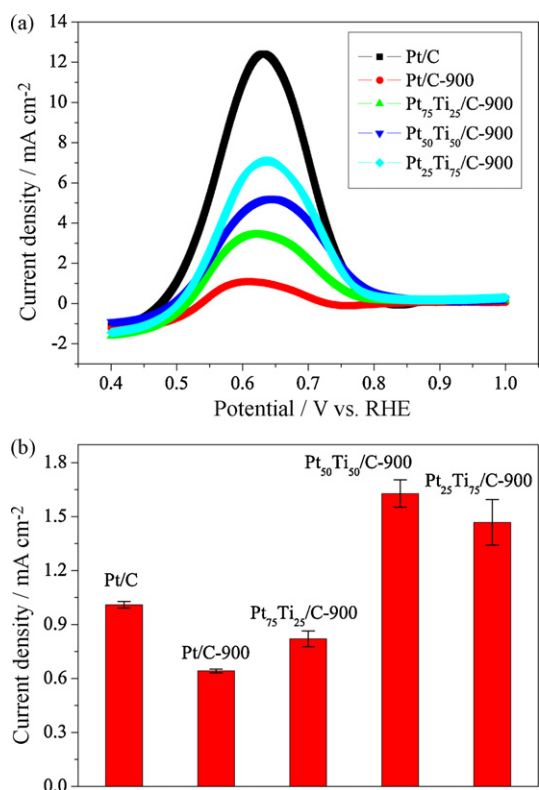
Fig. 5. (a) The RDE experiment results performed by cathodic potential sweep from 1.0 to 0.2 V at a scan rate of 5 mV s^{-1}. Oxygen purged 0.5 M H$_2$SO$_4$ + 0.1 M methanol solution was used as the electrolyte. Rotating speed of the RDE was 2000 rpm. (b) Current density decrease of the RDE caused by the presence of methanol during the ORR activity testing.

The effect of methanol on the ORR performance of these catalysts was also investigated, and the results are shown in Fig. 5(a). A large current density decrease was observed in all catalysts due to the MOR. The current density decrease due to the presence of methanol is shown in Fig. 5(b). At 0.8 V, the decrease of the ORR current densities were 1.01, 0.642, and 0.821 mA cm^{-2} for the Pt/C, Pt/C-900, and Pt$_{75}$Ti$_{25}$/C-900 catalysts, respectively. The current density drop was more significant in the Pt$_{50}$Ti$_{50}$/C-900 (1.63 mA cm^{-2}) and Pt$_{25}$Ti$_{75}$/C-900 (1.47 mA cm^{-2}) catalysts, which exhibited both high MOR and ORR activities. These results suggest that the alloyed Pt–Ti catalysts are not suitable as methanol-tolerant ORR catalyst due to their high MOR activity. A summary of electrochemical testing results is shown in Table 2.

4. Conclusion

The effect of Ti additions on the performance of Pt/C catalysts was investigated. After annealing at 900 °C for 30 min under H$_2$/Ar flow, formation of a Pt$_3$Ti phase was observed in the Pt$_{50}$Ti$_{50}$/C-900 and Pt$_{25}$Ti$_{75}$/C-900 catalysts. In the MOR, the Pt$_{50}$Ti$_{50}$/C-900 (87.4 mA mg$_{Pt}^{-1}$) and Pt$_{25}$Ti$_{75}$/C-900 (128 mA mg$_{Pt}^{-1}$) catalysts exhibited 103 and 198% higher mass activity, respectively, than the 43.0 mA mg$_{Pt}^{-1}$ value of the Pt/C-900 catalyst. These catalysts also showed higher ORR activity than Pt/C catalysts; specific ORR activity increased from 11.9 μA cm$_{Pt}^{-2}$ in the Pt/C catalyst to 32.3 and 30.2 μA cm$_{Pt}^{-2}$ in the Pt$_{50}$Ti$_{50}$/C-900 and Pt$_{25}$Ti$_{75}$/C-900 catalysts, respectively. The improved MOR and ORR activities of the Pt$_{50}$Ti$_{50}$/C-900 and Pt$_{25}$Ti$_{75}$/C-900 catalysts might come from the formation of Pt$_3$Ti phase or the presence of Ti oxide. However,

these catalysts suffered from poor ORR activity in the presence of methanol, which originated from high MOR activity.

References

[1] A.S. Arico, S. Srinivasan, V. Antonucci, Fuel Cells 1 (2001) 133–161.
[2] M. Watanabe, S. Motoo, J. Electroanal. Chem. 60 (1975) 267–273.
[3] N.M. Markovic, H.A. Gasteiger, P.N. Ross Jr., Electrochim. Acta 40 (1995) 91–98.
[4] W. Chrzanowski, A. Wieckowski, Langmuir 14 (1998) 1967–1970.
[5] O.A. Petrii, J. Solid State Electrochem. 12 (2008) 609–642.
[6] E. Antolini, Appl. Catal. B: Environ. 74 (2007) 324–336.
[7] C. Lamy, A. Lima, V. LeRhun, F. Delime, C. Coutanceau, J.-M. Léger, J. Power Sources 105 (2002) 283–296.
[8] U.B. Demirci, J. Power Sources 173 (2007) 11–18.
[9] M.K. Jeon, J.Y. Won, K.R. Lee, S.I. Woo, Electrochem. Commun. 9 (2007) 2163–2166.
[10] M.K. Jeon, K.R. Lee, H. Daimon, A. Nakahara, S.I. Woo, Catal. Today 132 (2008) 123–126.
[11] S. Pasupathi, V. Tricoli, J. Solid State Electrochem. 12 (2008) 1093–1100.
[12] J.S. Cooper, P.J. McGinn, J. Power Sources 163 (2006) 330–338.
[13] P. Strasser, Q. Fan, M. Devenney, W.H. Weinberg, P. Liu, J.K. Nørskov, J. Phys. Chem. B 107 (2003) 11013–11021.
[14] J.-H. Choi, K.-W. Park, B.-K. Kwon, Y.-E. Sung, J. Electrochem. Soc. 150 (2003) A973–A978.
[15] Z.B. Wang, G.P. Yin, P.F. Shi, Y.C. Sun, Electrochem. Solid-State Lett. 9 (2006) A13–A15.
[16] M.K. Jeon, J.S. Cooper, P.J. McGinn, J. Power Sources 185 (2008) 913–916.
[17] M.K. Jeon, K.R. Lee, K.S. Oh, D.S. Hong, J.Y. Won, S. Li, S.I. Woo, J. Power Sources 158 (2006) 1344–1347.
[18] M.K. Jeon, J.Y. Won, K.S. Oh, K.R. Lee, S.I. Woo, Electrochim. Acta 53 (2007) 447–452.
[19] P. Piela, C. Eickes, E. Brosha, F. Garzon, P. Zelenay, J. Electrochem. Soc. 151 (2004) A2053–A2059.
[20] Y. Chung, C. Pak, G.S. Park, W.S. Jeon, J.R. Kim, Y. Lee, H. Chang, D. Seung, J. Phys. Chem. C 112 (2008) 313–318.
[21] C. Roychowdhury, F. Matsumoto, V.B. Zeldovich, S.C. Warren, P.F. Mutolo, M.J. Ballesteros, U. Wiesner, H.D. Abruna, F.J. DiSalvo, Chem. Mater. 18 (2006) 3365–3372.
[22] S. Papadimitriou, A. Tegou, E. Pavlidou, G. Kokkinidis, S. Sotiropoulos, Electrochim. Acta 52 (2007) 6254–6260.
[23] H. Abe, F. Matsumoto, L.R. Alden, S.C. Warren, H.D. Abruna, F.J. DiSalvo, J. Am. Chem. Soc. 130 (2008) 5452–5458.
[24] L. Carrette, K.A. Friedrich, U. Stimming, Fuel Cells 1 (2001) 5–39.
[25] T. Toda, H. Igarashi, M. Watanabe, J. Electroanal. Chem. 460 (1999) 258–262.
[26] M. Wakisaka, H. Suzuki, S. Mitsui, H. Uchida, M. Watanabe, J. Phys. Chem. C 112 (2008) 2750–2755.
[27] V. Stamenkovic, T.J. Schmidt, P.N. Ross, N.M. Markovic, J. Phys. Chem. B 106 (2002) 11970–11979.
[28] S. Mukerjee, S. Srinivasan, J. Electroanal. Chem. 357 (1993) 201–224.
[29] U.A. Paulus, A. Wokaun, G.G. Scherer, T.J. Schmidt, V. Stamenkovic, V. Radmilovic, N.M. Markovic, P.N. Ross, J. Phys. Chem. B 106 (2002) 4181–4191.
[30] E. Ding, K.L. More, T. He, J. Power Sources 175 (2008) 794–799.
[31] J.A. Rodriguez, D.W. Goodman, Science 257 (1992) 897–903.
[32] U. Bardi, B.C. Beard, P.N. Ross, J. Catal. 124 (1990) 22–29.
[33] T. Toda, H. Igarashi, H. Uchida, M. Watanabe, J. Electrochem. Soc. 146 (1999) 3750–3756.
[34] S. Mukerjee, S. Srinivasan, M.P. Soriaga, J. Electrochem. Soc. 142 (1995) 1409–1422.
[35] M. Min, J. Cho, K. Cho, H. Kim, Electrochim. Acta 45 (2000) 4211–4217.
[36] M.M.P. Janssen, J. Moolhuysen, Electrochim. Acta 21 (1976) 869–878.
[37] A. Hamnett, B.J. Kennedy, S.A. Weeks, J. Electroanal. Chem. 240 (1988) 349–353.
[38] J. Shim, C.R. Lee, H.K. Lee, J.S. Lee, E.J. Cairns, J. Power Sources 102 (2001) 172–177.
[39] L. Xiong, A. Manthiram, Electrochim. Acta 49 (2004) 4163–4170.
[40] H. Liu, C. Song, L. Zhang, J. Zhang, H. Wang, D.P. Wilkinson, J. Power Sources 155 (2006) 95–110.
[41] K.L. Tsai, J.L. Dye, J. Am. Chem. Soc. 113 (1991) 1650–1652.
[42] B.C. Beard, P.N. Ross Jr., J. Electrochem. Soc. 133 (1986) 1839–1845.
[43] C.Z. He, H.R. Kunz, J.M. Fenton, J. Electrochem. Soc. 144 (1997) 970–979.
[44] T. Biegler, D.A.J. Rand, R. Woods, J. Electroanal. Chem. 29 (1971) 269–277.